Contents lists available at ScienceDirect

Digital Chinese Medicine

journal homepage: http://www.keaipublishing.com/dcmed

# Analysis on pulse features of coronary heart disease patients with or without a history of ischemic stroke

LI Xin†, LI Wei†, NG Man-In, PARRY Natalie Ann, LI Siqi, LI Rui, GUO Rui*

*School of Traditional Chinese Medicine, Shanghai University of Traditional Chinese Medicine, Shanghai 201203, China*

ARTICLE INFO

*Article history*
Received 28 July 2024
Accepted 05 September 2024
Available online 25 September 2024

*Keywords*
Pulse diagnosis
Coronary heart disease (CHD)
Ischemic stroke
Signal processing
Pattern recognition

ABSTRACT

**Objective** To evaluate the capability of wrist pulse analysis in distinguishing three physiological and pathological conditions: healthy individuals, coronary heart disease (CHD) patients without a history of ischemic stroke, and CHD patients with a history of ischemic stroke.

**Methods** Study participants were recruited from Shuguang East Hospital, Yueyang Hospital of Integrated Traditional Chinese and Western Medicine, and Shanghai Municipal Hospital of Traditional Chinese Medicine, affiliated with Shanghai University of Traditional Chinese Medicine, from April 15 to September 15, 2021. They were categorized into three groups: healthy controls (Group 1), CHD patients without a history of ischemic stroke (Group 2), and CHD patients with a history of ischemic stroke (Group 3). The wrist pulse signals of the study participants were non-invasively collected using a pulse diagnosis instrument. The linear time-domain features and nonlinear time-series multiscale entropy (MSE) features of the pulse signals were extracted using time-domain analysis and the MSE methods, which were subsequently compared between groups. Based on these extracted features, a recognition model was developed using a random forest (RF) algorithm. The classification performance of the models was evaluated using metrics, including accuracy, precision, recall, and F1-score derived from confusion matrix as well as the area under the receiver operating characteristics (ROC) curve (AUC).

**Results** A total of 189 participants were enrolled, with 63 in Group 1, 61 in Group 2, and 65 in Group 3. Compared with Group 1, Group 2 showed significant increases in pulse features H2/H1, H3/H1, W1, W2, and W2/T, and decreased in $MSE_1$ – $MSE_7$ ($P < 0.05$), while Group 3 showed significant increases in pulse features T5/T4, T, H1/T1, W1, W2, AS, and Ad, and decreased in $MSE_1$ – $MSE_{20}$ ($P < 0.05$). Compared with Group 2, Group 3 demonstrated notable increases in H1/T1 and As ($P < 0.05$). The RF model achieved precision of 80.00%, 61.54%, and 61.54%, recall of 74.29%, 60.00%, and 68.97%, F1-scores of 70.04%, 60.76%, and 65.04%, and AUC values of 0.92, 0.74, and 0.81 for Groups 1, 2, and 3, respectively. The overall accuracy was 67.69%, with micro-average AUC of 0.83 and macro-average AUC of 0.82.

**Conclusion** Differences in pulse features reflect variations in arterial compliance, peripheral resistance, cardiac afterload, and pulse signal complexity among healthy individuals, CHD

†The authors contributed equally.

*Corresponding author: GUO Rui, E-mail: guoruier@sina.com.

Peer review under the responsibility of Hunan University of Chinese Medicine.

DOI: 10.1016/j.dcmed.2024.12.006

**Citation:** LI X, LI W, NG MI, et al. Analysis on pulse features of coronary heart disease patients with or without a history of ischemic stroke. Digital Chinese Medicine, 2024, 7(3): 264-273.

patients without a history of ischemic stroke, and those with such a history. The developed pulse-based recognition model holds the potential in distinguishing between these three groups, offering a novel diagnostic reference for clinical practice.

## 1 Introduction

Cardiovascular diseases, predominantly driven by atherosclerosis, have emerged as the leading cause of death in China. This condition involves the narrowing and hardening of blood vessels caused by cholesterol deposition, which can potentially affect all parts of the arterial vascular system. Two significant consequences of atherosclerosis are coronary heart disease (CHD) and ischemic stroke, and there exists a notable degree of comorbidity between them [1]. Patients suffering both diseases can simultaneously experience severely compromised prognoses. One study showed that 43% to 85% of patients with ischemic stroke showed asymptomatic CHD, while 25% to 48% had severe CHD. Furthermore, ischemic stroke impacts the onset and progression of CHD [2]. A study by DUCROCQ et al. [3] that followed a total of 26 389 patients with CHD for four years demonstrated that a history of ischemic stroke increased the risk of recurrent cardiovascular events among CHD patients. Consequently, early diagnosis and treatment of one of the co-existing diseases, when patients are affected by both, may enhance their quality of survival and long-term prognosis. The most direct approach for detecting atherosclerotic disease could be through examining vascular lesions [4]. Although there are several clinical methods for the detection of angiopathy, such as angiography [5], their widespread use in disease prevention and monitoring is limited by factors such as invasiveness, delayed results, high cost, or complex operational procedures. This necessitates the exploration of a novel, noninvasive and user-friendly diagnostic tool that can effectively identify the status of CHD patients, particularly those who have experienced an ischemic stroke, thereby facilitating more precise and targeted interventions.

Traditional Chinese medicine (TCM) has long recognized the profound interconnection between the heart, brain, and blood vessels [6]. Within the holistic framework of TCM, the human body is viewed as an integrated entity, where various parts harmoniously coordinated in function, remain structurally inseparable, and exhibit pathologically interdependence. Blood vessels serve as the carriers for the functions and structures of both the heart and brain. Optimal cardiac governance of blood and vessels ensures clear passageways and unimpeded blood flow to the brain, thereby facilitating the brain's role in regulating the consciousness. Conversely, the heart's function is also influenced by the brain, establishing a bidirectional relationship. Therefore, the circulation of blood is indispensable for the normal functions of both the heart and brain [7]. Disruptions in blood flow lead to inadequate supply of blood and Qi to heart and brain, as a result of which cardiac and cerebral pathologies occur. "Chest impediment" and "ischemic stroke" exemplify such occurrences, coinciding with the modern medical understanding of the pathogenesis of cardiovascular and cerebrovascular diseases [8].

The consensus in modern medicine identifies atherosclerosis as the primary pathological factor underlying these conditions [9]. The progression of vascular lesions, whether in CHD or ischemic stroke, unfolds over an extended process. During the early or progressively worsening stages of the disease, hemodynamic parameters, including vascular elasticity, blood flow inertia, and blood pressure, undergo corresponding alterations. These changes are initially manifested in pulse wave propagating along the arterial tree. TCM pulse-taking offers a unique advantage in detecting the pulse wave at the radial artery, providing valuable insights into the confirmation of cardiovascular conditions.

Thus, the objective of this study is to analyze the pulse features of healthy individuals, patients with CHD but without a history of ischemic stroke, and patients who have experienced an ischemic stroke, with the aim of elucidating their physiological and pathological distinctions. Additionally, we strive to investigate the effectiveness of a model based on these pulse features for accurately distinguishing the distinct groups. Ultimately, our goal is to provide a valuable supplementary tool for the diagnosis and early warning of these comorbid conditions, thereby enhancing patients' prognostic outcomes.

## 2 Data and methods

### 2.1 Participants

This study recruited participants from April 15 to September 15, 2021, at three institutions affiliated with Shanghai University of Traditional Chinese Medicine: Shuguang East Hospital, Yueyang Hospital of Integrated Traditional Chinese and Western Medicine, and Shanghai Municipal Hospital of Traditional Chinese Medicine. Participants were categorized into three groups: healthy controls (Group 1), CHD patients without a history of ischemic stroke (Group 2), and CHD patients with a history of ischemic stroke (Group 3). All data were obtained with written informed consent from the participants and maintained under strict confidentiality protocols. This

study was approved by the Ethics Committee of Shanghai Municipal Hospital of Traditional Chinese Medicine (2022SHL-KY-15).

### 2.2 Diagnostic criteria

The diagnostic criteria for CHD referred to the guidelines issued by the American College of Cardiology [10]. The diagnostic criteria for ischemic stroke were based on the 2018 Guidelines for the Early Management of Patients with Acute Ischemic Stroke published by the American Heart Association and the American Stroke Association [11].

### 2.3 Inclusion and exclusion criteria for healthy individuals

**2.3.1 Inclusion criteria** (i) Individual must have a good health status, as determined by physical examination, with no history of major illnesses or conditions that could interfere with the study outcomes. (ii) Specific physiological indicators (such as blood pressure, blood glucose, and blood lipids) must be within normal ranges. (iii) Participants must be aged between 35 and 75 years. (iv) Complete basic information and clinical data must be available for each participant. (v) Individuals must demonstrate an understanding of the study objectives and procedures and provide written informed consent prior to participation.

**2.3.2 Exclusion criteria** (i) Individuals with severe chronic diseases such as cardiovascular disease, diabetes, cancer, or any other condition that could significantly impact the study outcomes. (ii) Individuals who have undergone major surgery or received significant treatment within the past six months. (iii) Individuals with a known history of drug allergy or a family history of specific diseases that could potentially interact with the study outcomes. (iv) Pregnant or breastfeeding women.

### 2.4 Inclusion and exclusion criteria for CHD patients

**2.4.1 Inclusion criteria** (i) Participants must have a confirmed diagnosis of CHD, with or without a history of ischemic stroke, as assessed and documented by a qualified cardiologist. (ii) Participants must be in good mental health, with no history of severe mental disorders, and capable of fully cooperating with the study procedures, including the collection process of clinical data. (iii) Participants must be aged between 35 and 75 years. (iv) Complete basic information and clinical data must be available for each participant. (v) Participants must demonstrate an understanding of the study objectives and procedures, and provide written informed consent prior to participation.

**2.4.2 Exclusion criteria** (i) Patients with cardiovascular disease other than CHD, including but not limited to aortic stenosis, myocardial infarction, arrhythmias, or heart failure. (ii) Patients with malignant tumors, active infectious diseases, or significant functional impairment of other organs, such as liver dysfunction and kidney dysfunction. (iii) Patients with a history of percutaneous coronary intervention (PCI) or coronary artery bypass grafting (CABG) prior to enrollment. (iv) Patients with significant neurological conditions affecting data collection, including but not limited to dementia, stroke with significant cognitive impairment, or other cognitive impairments that interfere with study procedures.

### 2.5 Data collection

**2.5.1 General information collection** The general information of participants, including gender, age, height, weight, body mass index (BMI), systolic blood pressure (SBP), diastolic blood pressure (DBP), past medical history, and other relevant details were collected. BMI was determined according to the formula: BMI = weight (kg)/[height (m)]$^2$. Blood pressure was measured with a sphygmomanometer.

**2.5.2 Pulse signals acquirement** Participants were instructed to adopt either supine or sitting position, with the forearm naturally extended forward and parallel to the heart. The wrist was straightened with the palm facing upwards and the fingers slightly curved. A small soft pillow was placed under the wrist joint to enhance the detection of pulse signals by facilitating the flow of local blood through the wrist. Prior to data collection, participants were required to remain stationary for a minimum of 3 min to ensure physiological stability. For the acquisition of pulse signals, the ZY-I type pulse diagnostic instrument was utilized, with focus on the left hand. The sampling frequency was set at 4 000 Hz, and the pulse signals under the optimal pressure section were selected for subsequent analysis of pulse features. This method allowed for the precise capture of pulse signals for further analysis.

### 2.6 Extraction of time-domain features from pulse signals

Pulse signals reflect the cardiac ejection activity and convey diverse information carried by pulse waves through the vascular system. Time-domain analysis primarily investigates the relationship between the amplitude and time of the waveform within a representative pulse signal cycle. This method extracts key characteristics of pulse waves, such as the peak heights (H) and the corresponding times (T), as illustrated in Figure 1 [12]. Based on the extracted peak and valley heights, as well as corresponding times, time-domain features are calculated to explore the intrinsic relationships between pulse features and diseased states. The pulse features are presented in Table 1.

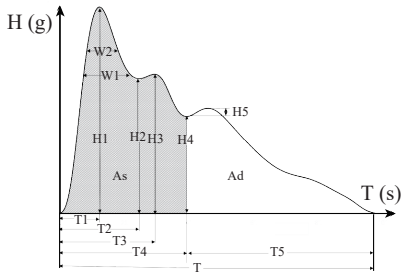


**Figure 1** One representative cycle of a pulse waveform

**Table 1** Time-domain features of the pulse signal

| Feature type | Feature parameter | Feature name |
|---|---|---|
| Amplitude | H1 | Main wave amplitude |
| | H2 | Main wave gorge amplitude |
| | H3 | Wave front dicrotic amplitude |
| | H4 | Dicrotic notch amplitude |
| | H5 | Dicrotic wave amplitude |
| | W1 | The width of main wave in its 1/3 height position |
| | W2 | The width of main wave in its 1/5 height position |
| Time | T1 | Main wave phase |
| | T2 | Main wave gorge phase |
| | T3 | Wave front dicrotic phase |
| | T4 | Dicrotic notch phase |
| | T5 | Dicrotic wave phase |
| | T | Pulse cycle |
| Proportion | H2/H1 | Main wave gorge to main wave amplitude ratio |
| | H3/H1 | Wave front dicrotic to main wave amplitude ratio |
| | H4/H1 | Dicrotic notch to main wave amplitude ratio |
| | H5/H1 | Dicrotic wave to main wave amplitude ratio |
| | T1/T | Main wave phase to pulse cycle ratio |
| | T1/T4 | Main wave phase to dicrotic notch phase ratio |
| | T5/T4 | Dicrotic wave phase to dicrotic notch phase ratio |
| | W1/T | Pulse width to pulse cycle ratio |
| | W2/T | Pulse width to pulse cycle ratio |
| | H1/T1 | Main wave amplitude to main wave phase ratio |
| Area | As | Systolic area |
| | Ad | Diastolic area |

To minimize the impact from manual operation during sampling, this study selected specific time-domain features of pulse signals for further analysis. These features include proportion features (H2/H1, H3/H1, H4/H1, H5/H1, H1/T1, T1/T, T1/T4, T4/T, T5/T4, W1/T, and W2/T), time-related features (T, W1, and W2), and area features (As and Ad).

## 2.7 Extraction of multiscale entropy from pulse signals

Multiscale entropy (MSE) extends the concept of sample entropy to encompass multiple time scales [13]. The traditional sample entropy overlooks the potential insights offered by analyzing different time scales within a given time series. Multiscale entropy addresses this limitation by computing sample entropy across various observational scales, enabling a more detailed analysis of pulse signals and the extraction of additional information.

Like other sample entropy measures, multiscale entropy serves as a valuable tool for assessing the complexity of time series data in medical research. Its fundamental principle involves coarse graining the time series, a process that involves averaging different numbers of consecutive data points to generate signals at distinct scales (resolutions). This approach facilitates the analysis of the time series at progressively coarser temporal scales. As illustrated in Figure 2 [14], at scale 1, the input data are the original time series. At scale 2, the coarse-grained time series is derived by averaging every two consecutive points from the original time series. Similarly, at scale 3, the coarse-grained time series is formed by averaging every three consecutive points from the original time series, and this pattern continues. For each respective scale, the sample entropy value is calculated for the coarse-grained time series at this specific scale.

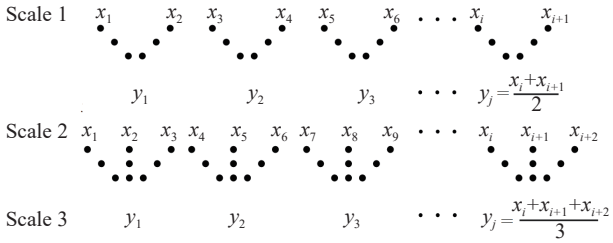


**Figure 2** The coarse-grained process of time series
*x*, original time series. *y*, coarse-grained time series.

The MSE values provide insights into the complexity of the time series at different temporal resolutions. Higher entropy values indicate greater complexity, while lower values suggest more regularity or predictability in the signal, making it a valuable tool for analyzing changes in the complexity of pulse signals at various temporal resolutions. In this study, we employed the MSE method to compute the sample entropy for each series at scale $i$ ($i$ = 1, 2, ..., 20), designated as $MSE_1$, $MSE_2$, $MSE_3$, ..., and up to $MSE_{20}$. We applied this approach to three distinct groups of pulse signals. This approach enabled us to effectively compare the signal complexity across the three groups.

## 2.8 Statistical methods

Data analysis was performed using SPSS 25.0 to compare pulse features and general information among the three

groups. For continuous variables that were not normally distributed, the Kruskal-Wallis $H$ test and the Nemenyi test were employed for comparisons, with data represented as the median [interquartile range (IQR)], denoted as M ($Q_1$, $Q_3$). For continuous variables that were normally distributed, analysis of variance (ANOVA) was used for comparisons, with data represented as mean ± standard deviation (SD). Categorical variables were compared using the Chi-squared test and expressed as percentages. $P < 0.05$ was considered statistically significant.

### 2.9 Establishment and evaluation of the model for three-group distinction

**2.9.1 Model establishment** Random forest (RF) is an ensemble learning algorithm that combines multiple classification decision trees [15]. It determines final classification outcome through a voting mechanism by aggregating the predictions of all individual decision trees. This collective model often exhibits superior prediction accuracy compared with traditional classification models, and has therefore been widely applied in bioinformatics, medicine, and other fields [16].

In this study, we utilized MATLAB 2015 (MathWorks Inc.) to implement the RF algorithm and to develop a classification model. This model was built using a dataset comprising pulse features and general clinical information from participants, with the aim of accurately categorizing samples into Group 1, Group 2, and Group 3. To enhance the model's predictive accuracy and optimize its training performance, we employed the synthetic minority over-sampling technique (SMOTE) [17] prior to model training to balance the sample size across groups. To ensure the objectivity and reliability of the model, we conducted a five-fold cross-validation on the dataset, where in each fold, 80% of data was randomly assigned as the training set for model training, while the remaining 20% was used as the testing set to validate the model's predictive performance. Through five rounds of iterative testing, we calculated the average prediction accuracy to comprehensively evaluate its classification capability.

**2.9.2 Model evaluation** A confusion matrix was utilized to evaluate the performance of prediction models by comparing the actual labels with the predicted ones. Key performance metrics such as accuracy, precision, recall, and F1-score were derived from this matrix to assess the model. These metrics are defined as follows.

(i) Accuracy. It represents the ratio of the number of correct predictions by the model to the total number of samples.

$$\text{Accuracy} = \frac{\text{Number of correct predictions}}{\text{Total number of samples}}$$

(ii) Precision. It indicates the proportion of true positive predictions among all positive predictions made by the model for a specific class $X$, it is calculated as:

$$\text{Precision} = \frac{\text{Number of true class } X \text{ predictions}}{\text{Total number of class } X \text{ predictions by the model}}$$

(iii) Recall. It is the proportion of true positive predictions out of all actual positive samples for a specific class $X$, it is calculated as:

$$\text{Recall} = \frac{\text{Number of true class } X \text{ predictions}}{\text{Total number of actual class } X \text{ samples}}$$

(iv) F1-score. This metric balances the model's precision and recall for each class $X$ and is computed as:

$$\text{F1-score} = \frac{2 \times (\text{Precision} \times \text{Recall})}{(\text{Precision} + \text{Recall})}$$

The receiver operating characteristics (ROC) curve is a fundamental tool for evaluating the performance of binary prediction models. A key metric derived from the ROC curve is the area under the curve (AUC), which quantifies the overall ability to distinguish between positive and negative classes. An AUC value closer to 1 indicates a highly effective prediction model.

For multi-class classification tasks or datasets with class imbalance, two approaches are commonly used to aggregate ROC performance: micro-average and macro-average. Micro-average ROC assesses model performance by combining all true positives, false positives, true negatives, and false negatives across all classes, treating each instance equally. Macro-average ROC, on the other hand, evaluates each class separately by calculating individual ROC curves and AUCs, and then averages them, ensuring that each class contributes equally to the final metric. This approach provides a more objective view on the model's overall performance.

In this study, we comprehensively evaluated the model's performance using a range of metrics, including accuracy, precision, recall, and F1-score. Additionally, we assessed the model's classification capability using the ROC curve, along with its AUC, micro-average AUC, and macro-average AUC.

## 3 Results

### 3.1 Comparison of general information among the three groups

A total of 235 participants were recruited for this study. However, only 189 remained following the inclusion and exclusion criteria and were categorized into three groups: Group 1 consisted of 63 healthy individuals, Group 2 comprised 61 patients diagnosed with CHD but without a history of ischemic stroke, and Group 3 included 65 CHD patients with a history of ischemic stroke.

As shown in Table 2, participants in Group 3 were significantly older compared with Group 1 and Group 2

($P < 0.05$), with the ages of participants in Group 2 being older compared with Group 1 ($P < 0.05$). In addition, the SBP of participants in Group 3 were significantly higher compared with Group 1 ($P < 0.05$), while no significant differences were observed in other parameters examined ($P > 0.05$).

### 3.2 Comparison of pulse features among the three groups

Statistical analysis was conducted on the time-domain features and MSE features extracted from the pulse signals of participants in the three groups (Table 3 and 4).

Significant differences in time-domain features were observed among the three groups (Table 3). Compared with Group 1, Group 2 exhibited significantly higher values for pulse features H2/H1, H3/H1, W1, W2, and W2/T ($P < 0.05$). Similarly, Group 3 demonstrated significantly elevated values for T5/T4, T, H1/T1, W1, W2, As, and Ad ($P < 0.05$). Moreover, when Group 3 compared with Group 2, significantly higher values were observed for H1/T1 and As ($P < 0.05$).

Table 4 revealed that Group 3 had significantly lower values for $MSE_1$ to $MSE_{20}$ compared with Group 1 ($P < 0.05$). Additionally, Group 2 demonstrated significantly lower values for $MSE_1$ to $MSE_7$ compared with Group 1 ($P < 0.05$).

### 3.3 Performance assessment of the prediction model

The RF model, constructed using datasets comprising the pulse time-domain features, MSE features, and general information, was comprehensively evaluated using a confusion matrix and ROC curves. Based on confusion matrix depicted in Figure 3A, the metrics of accuracy, precision, recall, and F1-score were calculated following the methodology outlined in Section 2.9.2. Additionally, ROC curves were used to further assess the performance of the

**Table 2** Comparison of general information among the three groups [*n* (%), mean ± SD]

| Group | Gender | | Age (year) | BMI (kg/m²) | SBP (mmHg) | DBP (mmHg) |
|---|---|---|---|---|---|---|
| | Male | Female | | | | |
| 1 | 27 (42.86) | 36 (57.14) | 50.85 ± 14.355 | 23.958 ± 2.757 | 127.82 ± 15.851 | 76.74 ± 12.653 |
| 2 | 23 (37.70) | 38 (62.30) | 61.89 ± 10.068▲ | 24.021 ± 4.258 | 132.33 ± 15.323 | 79.15 ± 9.748 |
| 3 | 34 (52.31) | 31 (47.69) | 71.92 ± 8.303▲* | 23.726 ± 2.830 | 137.68 ± 17.372▲ | 81.26 ± 9.902 |
| $x^2/F$ value | 2.814 | | 56.598 | 0.137 | 5.872 | 2.759 |
| *P* value | 0.245 | | < 0.001 | 0.872 | 0.003 | 0.066 |

▲$P < 0.05$, compared with Group 1. *$P < 0.05$, compared with Group 2.

**Table 3** Comparison of time-domain features of the pulse signals among the three groups [M (Q1, Q3)]

| Group | T | H1/T1 | As | Ad | H2/H1 |
|---|---|---|---|---|---|
| 1 | 0.738 (0.675, 0.807) | 14.433 (11.277, 17.450) | 174 553.5 (136 165, 202 218) | 64 361.85 (50 246, 78 674) | 0.892 (0.791, 0.945) |
| 2 | 0.761 (0.688, 0.876) | 15.723 (9.466, 21.573) | 198 407.0 (142 340, 274 594) | 82 709.10 (49 358, 125 825) | 0.944 (0.885, 0.973)▲ |
| 3 | 0.808 (0.726, 0.899)▲ | 19.716 (12.551, 27.547) *▲ | 262 886.0 (172 603, 349 526)*▲ | 85 683.50 (57 873, 135 087)▲ | 0.933 (0.814, 0.960) |
| *Z* value | 9.927 | 15.937 | 23.295 | 11.603 | 11.637 |
| *P* value | 0.007 | < 0.001 | < 0.001 | 0.003 | 0.003 |

| Group | H3/H1 | H4/H1 | H5/H1 | T1/T | T4/T |
|---|---|---|---|---|---|
| 1 | 0.725 (0.657, 0.814) | 0.400 (0.364, 0.459) | 0.377 (0.324, 0.433) | 0.150 (0.132, 0.174) | 0.423 (0.394, 0.455) |
| 2 | 0.816 (0.725, 0.889)▲ | 0.459 (0.352, 0.530) | 0.426 (0.317, 0.525) | 0.153 (0.126, 0.184) | 0.417 (0.384, 0.447) |
| 3 | 0.777 (0.685, 0.857) | 0.378 (0.309, 0.502) | 0.383 (0.328, 0.465) | 0.144 (0.125, 0.171) | 0.406 (0.376, 0.435) |
| *Z* value | 11.182 | 4.973 | 5.348 | 2.232 | 3.304 |
| *P* value | 0.004 | 0.083 | 0.069 | 0.328 | 0.192 |

| Group | T1/T4 | T5/T4 | W1 | W2 | W1/T | W2/T |
|---|---|---|---|---|---|---|
| 1 | 0.355 (0.322, 0.404) | 1.208 (1.162, 1.285) | 0.177 (0.152, 0.197) | 0.120 (0.106, 0.156) | 0.246 (0.214, 0.266) | 0.184 (0.141, 0.207) |
| 2 | 0.358 (0.313, 0.433) | 1.183 (1.108, 1.273) | 0.201 (0.165, 0.222)▲ | 0.161 (0.115, 0.174)▲ | 0.263 (0.231, 0.288) | 0.202 (0.170, 0.235)▲ |
| 3 | 0.343 (0.301, 0.392) | 1.166 (1.111, 1.219)▲ | 0.200 (0.174, 0.222)▲ | 0.153 (0.114, 0.183)▲ | 0.247 (0.212, 0.282) | 0.192 (0.145, 0.233) |
| *F* value | 1.779 | 8.029 | 11.592 | 9.854 | 5.598 | 7.757 |
| *P* value | 0.411 | 0.018 | 0.003 | 0.007 | 0.061 | 0.021 |

▲$P < 0.05$, compared with Group 1. *$P < 0.05$, compared with Group 2.

**Table 4** Comparison of MSE features of pulse signals among the three groups [M (Q1, Q3)]

| Group | $MSE_1$ | $MSE_2$ | $MSE_3$ | $MSE_4$ | $MSE_5$ |
|---|---|---|---|---|---|
| 1 | 0.042 (0.037, 0.047) | 0.085 (0.076, 0.095) | 0.131 (0.116, 0.147) | 0.176 (0.155, 0.198) | 0.217 (0.189, 0.242) |
| 2 | 0.036 (0.029, 0.045)▲ | 0.072 (0.058, 0.093)▲ | 0.111 (0.088, 0.143)▲ | 0.146 (0.120, 0.193)▲ | 0.183 (0.148, 0.234)▲ |
| 3 | 0.033 (0.028, 0.039)▲ | 0.067 (0.057, 0.080)▲ | 0.103 (0.087, 0.122)▲ | 0.139 (0.118, 0.163)▲ | 0.171 (0.147, 0.196)▲ |
| *Z* value | 31.823 | 31.812 | 31.993 | 31.208 | 29.43 |
| *P* value | < 0.001 | < 0.001 | < 0.001 | < 0.001 | < 0.001 |
| **Group** | **$MSE_6$** | **$MSE_7$** | **$MSE_8$** | **$MSE_9$** | **$MSE_{10}$** |
| 1 | 0.250 (0.214, 0.279) | 0.278 (0.236, 0.312) | 0.304 (0.254, 0.342) | 0.325 (0.274, 0.366) | 0.347 (0.292, 0.391) |
| 2 | 0.209 (0.170, 0.269)▲ | 0.240 (0.192, 0.305)▲ | 0.273 (0.211, 0.338) | 0.299 (0.229, 0.366) | 0.322 (0.242, 0.400) |
| 3 | 0.198 (0.170, 0.226)▲ | 0.224 (0.188, 0.250)▲ | 0.247 (0.205, 0.280)▲ | 0.271 (0.221, 0.307)▲ | 0.287 (0.237, 0.334)▲ |
| *Z* value | 25.826 | 22.231 | 18.936 | 17.16 | 14.924 |
| *P* value | < 0.001 | < 0.001 | < 0.001 | < 0.001 | 0.001 |
| **Group** | **$MSE_{11}$** | **$MSE_{12}$** | **$MSE_{13}$** | **$MSE_{14}$** | **$MSE_{15}$** |
| 1 | 0.369 (0.312, 0.412) | 0.388 (0.326, 0.435) | 0.408 (0.344, 0.461) | 0.427 (0.362, 0.483) | 0.439 (0.380, 0.503) |
| 2 | 0.342 (0.257, 0.437) | 0.359 (0.271, 0.471) | 0.38 5(0.284, 0.501) | 0.398 (0.297, 0.523) | 0.406 (0.309, 0.549) |
| 3 | 0.306 (0.250, 0.357)▲ | 0.324 (0.264, 0.379)▲ | 0.340 (0.279, 0.401)▲ | 0.354 (0.290, 0.424)▲ | 0.372 (0.306, 0.440)▲ |
| *Z* value | 14.256 | 12.896 | 12.122 | 11.626 | 11.384 |
| *P* value | 0.001 | 0.002 | 0.002 | 0.003 | 0.003 |
| **Group** | **$MSE_{16}$** | **$MSE_{17}$** | **$MSE_{18}$** | **$MSE_{19}$** | **$MSE_{20}$** |
| 1 | 0.462 (0.396, 0.523) | 0.472 (0.409, 0.545) | 0.500 (0.421, 0.573) | 0.515 (0.441, 0.594) | 0.518 (0.448, 0.611) |
| 2 | 0.423 (0.318, 0.570) | 0.446 (0.334, 0.596) | 0.468 (0.346, 0.622) | 0.475 (0.366, 0.634) | 0.494 (0.375, 0.667) |
| 3 | 0.387 (0.324, 0.461)▲ | 0.402 (0.330, 0.479)▲ | 0.417 (0.349, 0.500)▲ | 0.433 (0.351, 0.515)▲ | 0.441 (0.367, 0.539)▲ |
| *Z* value | 10.821 | 10.135 | 9.474 | 9.934 | 9.108 |
| *P* value | 0.004 | 0.006 | 0.009 | 0.007 | 0.011 |

▲$P < 0.05$, compared with Group 1.

model (Figure 3B). Table 5 summarized all the performance metrics, revealing F1-score values of 70.04%, 60.76%, and 65.04% for Group 1, Group 2, and Group 3, respectively, as well as AUC values of 0.92, 0.74, and 0.81 for the same groups. Furthermore, an accuracy of 67.69%, a micro-average AUC of 0.83, and a macro-average AUC of 0.82 provided a comprehensive evaluation of the model's overall performance across different groups.

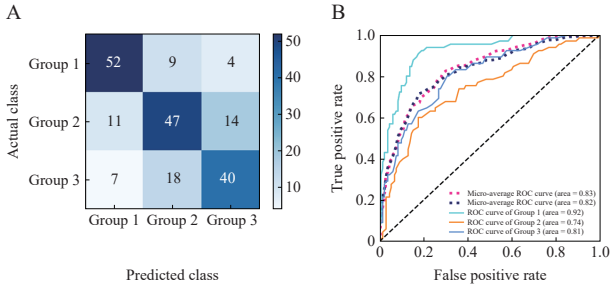


**Figure 3** Performance evaluation of the RF model

A, confusion matrix of the classification results. The darker color the more samples. B. ROC curves for the three groups.

## 4 Discussion

Atherosclerosis is a systemic disorder that affects multiple arterial segments, with CHD and ischemic stroke being two significant manifestations. These two conditions often coexist, significantly impacting patient outcomes [18]. Therefore, early diagnosis and treatment of ischemic stroke in patients with CHD can improve their quality of life and long-term prognosis.

Pulse diagnosis is an effective, noninvasive, convenient, and real-time diagnostic method for assessing arterial structures and functions [19]. Despite research focusing on cardiocerebral diseases, studies that distinguish wrist pulse signals between CHD patients without a history of ischemic stroke and those with such a history remain scarce. Consequently, our study compared and

**Table 5** Evaluation metrics of the RF model for the three groups

| Group | Precision (%) | Recall (%) | F1-score (%) | AUC | Accuracy (%) | Micro-average AUC | Macro-average AUC |
|---|---|---|---|---|---|---|---|
| 1 | 80.00 | 74.29 | 70.04 | 0.92 | | | |
| 2 | 61.54 | 60.00 | 60.76 | 0.74 | 67.69 | 0.83 | 0.82 |
| 3 | 61.54 | 68.97 | 65.04 | 0.81 | | | |

analyzed time-domain and MSE features of pulse signals extracted from healthy individuals, CHD patients without a history of ischemic stroke, and those with a history of ischemic stroke. By distinguishing the pathological states of the three populations using their pulse signals, we aim to provide novel insights that could inform clinical diagnosis and treatment strategies.

### 4.1 Comparative analysis of pulse features for distinct groups

Our findings were summarized as follows. Upon analyzing general clinical information, we observed that CHD patients without a history of ischemic stroke and those with such a history were significantly older compared with healthy individuals. Additionally, CHD patients with a history of ischemic stroke exhibited higher systolic blood pressure than healthy individuals. These findings are consistent with the widely recognized knowledge that advanced age and hypertension constitute significant risk factors for atherosclerosis [20] . This suggests that CHD patients with a history of ischemic stroke may have a heavier atherosclerotic burden and increased risk for cardiovascular and cerebrovascular events. It is important to note that both blood pressure and age can influence pulse waveforms by affecting the deformation of the vascular wall and altering the dynamics of blood flows [21]. Therefore, when developing diagnostic models based on pulse signals, it is essential to take these factors into consideration to enhance the accuracy and reliability of the models.

Furthermore, a comparative analysis of the time-domain features of wrist pulse signals among the three groups revealed several significant findings. (i) Compared with healthy controls, CHD patients without a history of ischemic stroke exhibited higher ratios of H2/H1, H3/H1, W1, W2, and W2/T, indicating poorer arterial compliance, increased peripheral resistance, prolonged hypertension duration, and augmented cardiac afterload [22]. (ii) Compared with the healthy controls, CHD patients with a history of ischemic stroke exhibited elevated values for T5/T4, T, H1/T1, W1, W2, As, and Ad. This result indicates that the pathological changes in CHD patients with an ischemic stroke history are characterized by enhanced myocardial contractility, a slower heart rate, prolonged hypertension duration, and increased cardiac output during both the systolic and diastolic phases [22]. These alterations carry specific pathophysiological significance, particularly markedly elevated SBP in this patient group. Under hypertensive conditions, the heart may adapt by enhancing myocardial contractility and reducing heart rate to maintain adequate cardiac output and stabilize blood pressure, thereby counteracting the increased peripheral resistance. However, the prolonged persistence of these adaptive changes may ultimately exert adverse effects on cardiac health. (iii) When compared with CHD patients without a history of ischemic stroke, those with such a history exhibited greater values for As and H1/T, suggesting an increase in myocardial contractility and systolic cardiac output. These alterations represent an adaptive response of the body to ischemic stroke and myocardial ischemia. This adaptation helps maintain stable blood pressure and cardiac output, thereby ensuring adequate blood supply to vital organs. Nonetheless, the persistence of these adaptive changes over time may lead to adverse consequences for the heart, such as the gradual progression of myocardial hypertrophy to heart failure, and the acceleration of coronary atherosclerosis due to persistent hypertension combined with enhanced myocardial contractility, ultimately resulting in more serious myocardial ischemia events.

Regarding the MSE features, our analysis also revealed significant differences among the different groups. Specifically, MSE values spanning both larger and smaller scales ($MSE_1$ – $MSE_{20}$) were significantly lower in CHD patients with a history of ischemic stroke compared to healthy controls. Similarly, MSE values in larger scales ($MSE_1$ – $MSE_7$) were also reduced in CHD patients without a history of ischemic stroke when compared with the controls. These findings reflect the reduced complexity of pulse signals in pathological states, with the most pronounced decrease observed in CHD patients who have suffered from ischemic stroke. MSE serves as a quantitative metric of irregularity or complexity of pulse signals, with lower values signifying reduced complexity and increased regularity, which is correlated with the diseased states [21]. In this context, the decreased MSE values observed in CHD patients, particularly those with a past ischemic stroke, may reflect the underlying pathophysiological mechanisms related to both cardiovascular and cerebrovascular systems, such as impaired autonomic regulation or vascular dysfunction, both of which are commonly associated with CHD and ischemic stroke. To further our understanding of these findings, additional research is needed to elucidate the precise mechanisms underlying these MSE changes and to explore their potential implications for disease progression.

### 4.2 Model performance analysis and future prospects

Our study comprehensively analyzed both linear and nonlinear characteristics of pulse signals and developed a classification model based on time-domain and MSE features. For the healthy individuals (Group 1), the model's performance metrics precision, recall, F1-score, and AUC were optimal, reaching 80.00%, 74.29%, 70.04%, and 0.92, respectively. However, for CHD patients without a history of ischemic stroke (Group 2) and those with a history of ischemic stroke (Group 3), these metrics exhibited a

decline. This decrease might be attributed to the overlapping pathological foundations between Group 2 and Group 3, posing a challenge on differentiating their pathological states. Despite this challenge, the model's overall prediction accuracy remained at 67.69%, indicating its ability to discern between different pathological states to some extent. Furthermore, the proximity of the micro-average and macro-average AUC values suggested that the model demonstrated a relatively consistent performance across all groups, despite variations observed in its performance on healthy individuals. This consistency is a positive indicator of the model's robustness and generalizability. Collectively, our findings have confirmed the feasibility of using pulse signals to classify the different pathological states in humans.

However, the findings of this study are inherently constrained by the limited sample size, which restricts the model's generalization ability and its extensive application. This constraint might lead to overfitting, causing the model to perform poorly on more diverse or unfamiliar data. Furthermore, despite our consideration of both linear and nonlinear features, there remains possible that some crucial features have been overlooked, potentially affecting the model's accuracy and robustness. Additionally, improper setting of model parameters poses another obstacle to enhancing the performance of the model.

For future research, first, we should augment the sample size and diversity to ensure the balance and representativeness of the study results, thereby enhancing the model's generalization capacity. Second, we need to deepen feature research by constructing features closely related to the problem domain, enhancing the model's learning ability. Third, we should integrate multimodal information, encompassing other diagnostic data from both Chinese medicine and Western medicine, to improve the accuracy and reliability of the prediction model. Last, we should also strive to optimize the model's training parameters, balancing predictive performance and model simplicity. Through these efforts, we aspire to develop a more accurate, robust, and widely applicable model for real-world clinical scenarios.

## 5 Conclusion

Differences in pulse features reflect variations in arterial compliance, peripheral resistance, and cardiac afterload, as well as the complexity of pulse signals among healthy individuals, CHD patients without a history of ischemic stroke, and those with such a history. The pulse-based recognition model holds potential in differentiating the three populations, offering a novel diagnostic reference for clinical practice.

## Findings

National Natural Science Foundation of China (82074332), Shanghai Key Laboratory of Health Identification and Assessment (21DZ2271000), and the 14th Batch of Science and Innovation Program for Undergraduates (202110268031).

## Competing interests

The authors declare no conflict of interest.

## References

[1] BENJAMIN EJ, BLAHA MJ, CHIUVE SE, et al. Heart disease and stroke statistics-2017 update: a report from the American Heart Association. Circulation, 2017, 135(10): e146–e603.

[2] LEE JW, HUR J, CHOI SI, et al. Incremental prognostic value of computed tomography in stroke: rationale and design of the IMPACTS study. The International Journal of Cardiovascular Imaging, 2016, 32: 83–89.

[3] DUCROCQ G, AMARENCO P, LABREUCHE J, et al. A history of stroke/transient ischemic attack indicates high risks of cardiovascular event and hemorrhagic stroke in patients with coronary artery disease. Circulation, 2013, 127(6): 730–738.

[4] KHANDELWAL P, YAVAGAL DR, SACCO RL. Acute ischemic stroke intervention. Journal of the American College of Cardiology, 2016, 67(22): 2631–2644.

[5] YOKO K, BHARATH A, YOSHIMORI K, et al. Non-contrast coronary magnetic resonance angiography: current frontiers and future horizons. Magma, 2020, 33(5): 1–22.

[6] LIU S, ZHU JJ, LI JC. The interpretation of human body in traditional Chinese medicine and its influence on the characteristics of TCM theory. Anatomical Record, 2021, 304(11): 2559–2565.

[7] BOS D, ARSHI B, VAN DEN BOUWHUIJSEN QJA, et al. Atherosclerotic carotid plaque composition and incident stroke and coronary events. Journal of the American College of Cardiology, 2021, 77(11): 1426–1435.

[8] YANG L, WANG CX. Evolution of the disease name of thoracic paralytic heartache. Journal of Changchun University of Traditional Chinese Medicine, 2020, 36(5): 854–857.

[9] FAN JL, WATANABE T. Atherosclerosis: known and unknown. Pathology International, 2022, 72(3): 151–160.

[10] Writing Committee Members; VIRANI SS, NEWBY LK, ARNOLD SV, et al. 2023 AHA/ACC/ACCP/ASPC/NLA/PCNA Guideline for the Management of Patients With Chronic Coronary Disease: A Report of the American Heart Association/American College of Cardiology Joint Committee on Clinical Practice Guidelines. American College of Cardiology, 2023, 82(18): 1808.

[11] POWERS WJ, RABINSTEIN AA, ACKERSON T, et al. 2018 Guidelines for the Early Management of Patients with Acute Ischemic Stroke. The American Heart Association/The American Stroke Association, 2018, 49(3): e46–e110.

[12] BUSA MA, VAN EMMERIK REA. Multiscale entropy: a tool for understanding the complexity of postural control. Journal of Sport and Health Science, 2016, 5(1): 44–51.

[13] FEI ZF, XU JT. Pulse Diagnosis in Chinese Medicine. Beijing: People's Medical Publishing House, 2009.
[14] COSTA M, GOLDBERGER AL, PENG CK. Multiscale entropy analysis of complex physiologic time series. Physical Review Letters, 2002, 89(6): 068102.
[15] CHEN HY, HE Y. Machine learning approaches in traditional Chinese medicine: a systematic review. The American Journal of Chinese Medicine, 2022, 50(1): 91–131.
[16] HU JC, SZYMCZAK S. A review on longitudinal data analysis with random forest. Briefings in Bioinformatics, 2023, 24(2): bbad002.
[17] FERNÁNDEZ A, GARCÍA S, HERRERA F, et al. SMOTE for learning from imbalanced data: progress and challenges, marking the 15-year anniversary. Journal of Artificial Intelligence Research, 2018, 61: 863–905.
[18] BEBO A, JARMUL JA, PLETCHER MJ, et al. Coronary heart disease and ischemic stroke polygenic risk scores and atherosclerotic cardiovascular disease in a diverse, population-based cohort study. PLoS One, 2023, 18(6): e0285259.
[19] HUANG JL, LIANG MC, TANG Y, et al. Application progress of digital pulse diagnosis technology in cardiovascular diseases. Chinese Journal of Information on Traditional Chinese Medicine, 2024, 31(7): 193–197.
[20] YONEYAMA K, GJESDAL O, CHOI EY, et al. Age, sex, and hypertension-related remodeling influences left ventricular torsion assessed by tagged cardiac magnetic resonance in asymptomatic individuals: the multi-ethnic study of atherosclerosis. Circulation, 2012, 126(21): 2481–2490.
[21] CUI J, SONG LC. Wrist pulse diagnosis of stable coronary heart disease based on acoustics waveforms. Computer Methods and Programs in Biomedicine, 2022, 214: 106550.
[22] LIU L, ZHANG CK, YAN JJ, et al. Analysis of characteristics of pulse-graph parameters in patients with different degree of coronary artery occlusion. Journal of Beijing University of Traditional Chinese Medicine, 2022, 45(8): 835–841.

# 冠心病伴或不伴缺血性卒中病史患者的脉象特征分析

李欣†, 李伟†, 吴文妍, 彭詠捷, 李思琪, 黎瑞, 郭睿*

*上海中医药大学中医学院, 上海 201203, 中国*

**【摘要】目的** 评估脉图分析技术在识别健康人群、冠心病（CHD）患者不伴以及伴缺血性卒中病史的三类不同生理病理状态人群的应用潜力。**方法** 于 2021 年 4 月 15 日至 9 月 15 日在上海中医药大学附属曙光医院东院、岳阳中西医结合医院以及上海市中医医院招募研究对象，并将他们分为三组：健康对照组（组 1）、无缺血性卒中史的 CHD 患者（组 2）和有缺血性卒中史的 CHD 患者（组 3）。应用脉诊仪无创采集脉象信号，运用时域分析和多尺度熵（MSE）方法提取脉象信号的线性时域特征和非线性时间序列 MSE 特征，并进行组间比较分析。基于这些脉象特征，运用随机森林（RF）算法建立识别模型。采用混淆矩阵计算的准确率、精确率、召回率、F1 分数以及受试者工作特征曲线下（ROC）面积（AUC）等指标评估模型的分类性能。**结果** 最终纳入 189 名受试者，其中组 1 共 63 例，组 2 共 61 例，组 3 共 65 例。与组 1 相比，组 2 脉象特征 H2/H1、H3/H1、W1、W2 和 W2/T 均显著升高，其 $MSE_1$ – $MSE_7$ 显著降低（$P < 0.05$），组 3 脉象特征 T5/T4、T、H1/T1、W1、W2、AS 和 Ad 均显著升高，其 $MSE_1$ – $MSE_{20}$ 显著降低（$P < 0.05$）；与组 2 相比，组 3 的 H1/T1 和 As 值显著升高（$P < 0.05$）。RF 模型对组 1、2、3 的识别精确率分别为 80.00%、61.54%、61.54%，召回率分别为 74.29%、60.00%、68.97%，F1 值分别为 70.04%、60.76%、65.04%，AUC 值分别为 0.92、0.74、0.81。模型总体准确率为 67.69%，微观平均 AUC 为 0.83，宏观平均 AUC 为 0.82。**结论** 脉象特征差异体现了健康人群、无缺血性卒中病史的 CHD 患者以及有缺血性卒中病史的 CHD 患者在动脉顺应性、外周阻力、心脏后负荷以及脉象信号系统复杂性存在的差异。基于脉象的识别模型在区分这三类人群上展现了良好潜力，有望为临床实践提供新的参考依据。

**【关键词】**脉诊；冠心病；缺血性脑梗死；信号处理；模式识别